

# The process of somatic hypermutation increases polyreactivity for central nervous system antigens in primary central nervous system lymphoma

Manuel Montesinos-Rongen,<sup>1</sup> Monica Terrao,<sup>1</sup> Caroline May,<sup>2</sup> Katrin Marcus,<sup>2</sup> Ingmar Blümcke,<sup>3</sup> Martin Hellmich,<sup>4</sup> Ralf Küppers,<sup>5</sup> Anna Brunn<sup>1</sup> and Martina Deckert<sup>1</sup>

<sup>1</sup>Institute of Neuropathology, Faculty of Medicine and University Hospital Cologne, University of Cologne, Cologne; <sup>2</sup>Medizinisches Pro-  
teom-Center, Ruhr-University Bochum, Bochum; <sup>3</sup>Department of Neuropathology, University Hospital Erlangen, Erlangen, Germany; <sup>4</sup>In-  
stitute of Medical Statistics and Computational Biology (IMSB), Faculty of Medicine and University Hospital Cologne, University of  
Cologne, Cologne and <sup>5</sup>Institute of Cell Biology (Cancer Research), University of Duisburg-Essen, Medical School, Essen, Germany, and  
German Cancer Consortium (DKTK), Essen/Düsseldorf, Germany

©2021 Ferrata Storti Foundation. This is an open-access paper. doi:10.3324/haematol.2019.242701

Received: November 8, 2019.

Accepted: March 18, 2020.

Pre-published: March 19, 2020.

Correspondence: MARTINA DECKERT - [martina.deckert@uni-koeln.de](mailto:martina.deckert@uni-koeln.de)

---

**Title:** The process of somatic hypermutation increases polyreactivity for central nervous system antigens in primary central nervous system lymphoma.

**Authors:** Manuel Montesinos-Rongen<sup>1</sup>, Monica Terrao<sup>1</sup>, Caroline May<sup>2</sup>, Katrin Marcus<sup>2</sup>, Ingmar Blümcke<sup>3</sup>, Martin Hellmich<sup>4</sup>, Ralf Küppers<sup>5</sup>, Anna Brunn<sup>1</sup>, and Martina Deckert<sup>1</sup>

**Affiliations:** <sup>1</sup>Institute of Neuropathology, Faculty of Medicine and University Hospital Cologne, University of Cologne, Cologne, Germany;

<sup>2</sup>Medizinisches Proteom-Center, Ruhr-University Bochum, Bochum, Germany;

<sup>3</sup>Department of Neuropathology, University Hospital Erlangen, Erlangen, Germany;

<sup>4</sup>Institute of Medical Statistics and Computational Biology (IMSB), Faculty of Medicine and University Hospital Cologne, University of Cologne, Cologne, Germany;

<sup>5</sup>Institute of Cell Biology (Cancer Research), University of Duisburg-Essen, Medical School, Essen, Germany, and German Cancer Consortium (DKTK)

## Supplemental Material

## **Supplemental Methods**

### **Assessment of autoreactivity by indirect immunofluorescence with HEp-2 cells, anti-nuclear antibody (ANAcombi) ELISA and anti-nuclear and cellular antibody (ANCAcombi) ELISA**

RecAb (ELISA: 200 ng/ $\mu$ l, HEp-2: 250 ng/ $\mu$ l as well as 10  $\mu$ g/ml), were tested by ANAcombi and ANCAcombi ELISA and with the HEp-2 kit (Orgentec, Mainz, Germany Assays) according to the manufacturer's instructions.

### **Determination of recAb reactivity against spliceosomal nuclear ribonucleoprotein C (SNRPC) by ELISA**

Recombinant human SNRPC (OriGene, Herford, Germany) was coated (5  $\mu$ g/ml) to a 96 well plate (Eppendorf, Hamburg, Germany) at 4°C overnight. After blocking (1% BSA in PBS-T), recAbs (200  $\mu$ g/ml as well as 10  $\mu$ g/ml) were applied, followed by donkey anti-rabbit IgG alkaline phosphatase (1:5,000, Jackson ImmunoResearch, Cambridgeshire, UK). Monoclonal rabbit anti-human SNRPC (clone EPR16034, Abcam, Cambridge) monoclonal mouse anti-MBP antibody (clone MBP101, Abcam) was used as positive control and negative control, respectively (400 ng/ml). Analysis was performed in triplicate. Experiments were repeated twice.

### **Immunoprecipitation of nBCR and tBCR with non-tumor CNS tissue**

Twenty 10  $\mu$ m frozen sections from brain biopsies of five epilepsy patients were lysed with RIPA buffer (Sigma, Deisenhofen, Germany) and pooled. Immunoprecipitation with purified recAb (5  $\mu$ g) was performed according to the manufacturer (Miltenyi Biotech, Bergisch Gladbach, Germany). Proteins were eluted with Laemmli buffer, separated by SDS-PAGE (with proteins migrating up to 1 cm), and analysed by mass spectrometry. Immunoprecipitation in the absence of antibody served as control (10

replicates). RecSA13 was used as control (5 µg/ml). Cut-off for immunoprecipitated proteins was > 2-fold enrichment. Only proteins that yielded consistently positive results in triplicate analyses were considered.

### **Immunoprecipitation of nBCR and tBCR with PCNSL**

Twenty 10 µm frozen sections from cryopreserved PCNSL (cases #01, #02, #03, #04, #05, #08, #09, #10) were lysed with 250 µl of RIPA buffer (Sigma). Immunoprecipitation was performed with recAbs (5 µg) and 25 µl of µMACS ProteinG MicroBeads (Milteny) according to the manufacturer's instructions. Proteins bound were eluted with Laemmli buffer and separated by SDS-PAGE with proteins migrating up to 1 cm. Gel segments containing the proteins were dissected and analysed by mass spectrometry. Immunoprecipitation in the absence of recAb served as control. Cut-off for immunoprecipitated proteins was > 2-fold enrichment. Only proteins that yielded consistent positive results in triplicate analyses were considered.

### **Semiquantitative evaluation of SNRPC expression**

Immunohistochemical expression of SNRPC (clone EPR16034, Abcam) was evaluated (PCNSL #11-#30) according to a semiquantitative grading system (0: no cells, +:>0–30%, ++:>30–50%, +++:>50–80%, ++++:>80–100% of cells independently by two authors (M.D., A.B.), yielding similar results.

### **Double immunofluorescence for neurabin-I and Neu-N**

Paraffin sections of normal brain were stained with mouse anti-human NeuN (clone A60, Merck Millipore, Darmstadt, Germany), horse anti-mouse BSP (Dianova, Hamburg, Germany), and extravidin-FITC (Sigma, Deisenhofen, Germany), followed

by rabbit anti-neurabin-I antibody (ab3483, Abcam, Cambridge, UK) and goat anti-rabbit-Cy3 (Dianova). As negative control, primary antibodies were omitted.

**Supplemental Table 1: Patients' data.**

<b>PCNSL #</b>	<b>Sex</b>	<b>Age</b>	<b>Analysis</b>
01	male	74	recAb
02	male	63	recAb
03	male	71	recAb
04	female	74	recAb
05	male	69	recAb
06	male	59	recAb
07	female	51	recAb
08	male	54	recAb
09	female	73	recAb
10	male	71	recAb
11	male	73	Immunohistochemistry
12	female	73	Immunohistochemistry
13	female	76	Immunohistochemistry
14	male	79	Immunohistochemistry
15	female	66	Immunohistochemistry
16	male	69	Immunohistochemistry
17	male	78	Immunohistochemistry
18	male	47	Immunohistochemistry
19	female	80	Immunohistochemistry
20	female	70	Immunohistochemistry
21	female	71	Immunohistochemistry
22	female	69	Immunohistochemistry

23	female	76	Immunohistochemistry
24	male	79	Immunohistochemistry
25	male	86	Immunohistochemistry
26	male	60	Immunohistochemistry
27	male	66	Immunohistochemistry
28	female	69	Immunohistochemistry
29	female	77	Immunohistochemistry
30	female	75	Immunohistochemistry
31	female	77	Western blot
32	female	77	Western blot
33	female	69	Western blot
34	female	67	Western blot
35	female	76	Western blot
36	female	76	Western blot
37	female	70	Western blot
38	female	79	Western blot
39	male	65	Western blot
40	male	63	Western blot
41	male	66	Western blot
42	female	61	Western blot
43	female	80	Western blot
44	male	74	Western blot
45	male	71	Western blot
46	male	60	Western blot
47	female	79	Western blot

48	female	77	Western blot
49	female	63	Western blot
50	female	57	Western blot

All patients were HIV-negative. Systemic lymphoma manifestation was excluded.



**Supplemental Table 2:** Immunoglobulin heavy and light gene characteristics of the PCNSL used for generation of naive BCR.

case	heavy chain				light chain		
	IGHV	IGHD	IGHJ	mutation frequency	IGK/JV	IGK/JL	mutation frequency
#01	IGHV3-23	IGHD3-16	IGHJ6	6.25	IGKV2-28	IGKJ1	6.12
#02	IGHV3-30	IGHD2-15	IGHJ4	7.64	IGLV1-47	IGLJ3	3.16
#03	IGHV3-48	IGHD6-19	IGHJ4	11.81	IGKV4-1	IGKJ1	14.48
#04	IGHV3-7	IGHD2-2	IGHJ4	2.08	IGKV2-30	IGJKJ1	5.68
#05	IGHV3-74	IGHD1-26	IGHJ4	14.93	IGKV2-28	IGKJ4	7.48
#06	IGHV4-34	IGHD4-23	IGHJ5	15.09	IGLV1-40	IGLJ2	11.46
#07	IGHV4-34	IGHD2-8	IGHJ5	14.44	IGLV1-40	IGLJ1	10.42
#08	IGHV4-34	IGHD6-25	IGHJ4	5.96	IGKV1-39	IGKJ2	13.62
#09	IGHV4-34	IGHD3-16	IGHJ3	12.28	IGKV1-5	IGKJ2	8.24
#10	IGHV4-34	IGHD1-26	IGHJ5	8.42	IGKV2-40	IGKJ1	2.69

**Supplemental Table 3:** Immunoglobulin heavy and light chain sequences.

As separate Excel file.

**Supplemental Table 4:** The recombinant anti-tetanus toxoid antibody recSA13 recognizes tetanus toxoid protein as dominant target in immunoprecipitation with epilepsy tissue and tetanus toxoid.

As separate Excel file.

**Supplemental Table 5:** Results of ProtoArray analysis.

As separate Excel file.

**Supplemental Table 6:** Results of immunoprecipitation analysis.

As separate Excel file.

**Supplemental Table 7:** Expression of SNRPC in PCNSL.

PCNSL #	SNRPC
11	++++
12	++++
13	+
14	+++
15	+
16	+
17	++++
18	+
19	++++
20	++++
21	++
22	++++
23	++++
24	++++
25	+++
26	+++
27	+
28	++++
29	++++
30	++++

0, no expression;

+, > 0 – 30 % of tumor cells immunoreactive;

++, > 30 – 50 % of tumor cells immunoreactive;

+++, > 50 – 80 % of tumor cells immunoreactive;

++++, > 80 – 100 % of tumor cells immunoreactive.

## Supplemental Figure Legends

### Supplemental Figure 1 Generation of recAbs

A: For each recAb (3 µg), expression of the heavy (~56 KDa) and light chain (25-30 KDa) is demonstrated by SDS-PAGE.

B, C: To test for potentially functional folding, reactivity of the recAbs with anti-human IgG was studied by ELISA. The initial concentration was 10 ng/µl for each recAb. Human IgG (initial concentration: 10 ng/µl) was used as positive control (B,C), and anti-SNRPC (Abcam) was used as negative control (C). Data are shown for nBCR and tBCR of PCNSL #09 and #10 (B) and for PCNSL #02 (C). Similar results were obtained for all recAbs. Each experiment was performed in triplicate; standard deviation is given for each point of measurement.

### Supplemental Figure 2 Regular staining staining pattern of the antibodies used for protein expression analysed in appropriate positive control tissues

A: Nuclear expression of SNRPC (Cy3) in nuclei of seminal epithelium of a normal testis. Staining with monoclonal rabbit anti-SNRPC (clone EPR16034, Abcam).

B: Selective, prominent expression of the CD20 antigen (FITC) on the surface of malignant B cells of a PCNSL. Staining with monoclonal mouse anti-CD20 (clone L26, DCS).

C: In an inflammatory, demyelinating brain lesion macrophages (arrowheads) and activated microglial cells (arrows) prominently express the CD68 antigen (FITC). Staining with monoclonal mouse anti-CD68 (clone CS, PG-M1, DCS).

D: In the normal temporal cortex, neurons express NeuN in the nuclei (FITC). Staining with monoclonal mouse anti-NeuN (clone A60, Millipore).

E: Activated astrocytes in the temporal grey matter express GFAP (arrows, FITC). Staining with monoclonal mouse anti-GFAP (clone GA-5, BioGenex).

F: In an anaplastic oligodendroglioma (WHO grade III), the tumor cells show a nuclear expression of Olig2 (FITC). Staining with monoclonal mouse anti-Olig2 (clone Olig2/2400, Abcam).

G: Capillary endothelial cells express the CD34 antigen (arrows, FITC). \* indicates the vascular lumen. Staining with monoclonal mouse anti-CD34 (clone QBend/10, BioGenex).

Microphotographs were taken with an Axiophot (Zeiss, Jena, Germany) and Zen 2 software (Zeiss). Original magnification: x400 (objective: x40). Adjustment for contrast and brightness were performed with Adobe Photoshop software version CC.

**Supplemental Figure 3** Absence of staining with omission of the primary antibodies used for protein expression analysed in appropriate positive control tissues

A: Omission of the CD20 (FITC) and the SNRPC (Cy3) antibodies abolishes immunostaining of the CD20<sup>+</sup> SNRPC<sup>+</sup> tumor cells of a PCNSL.

B: Macrophages/activated microglia intermingled between the tumor cells of a PCNSL are not stained when the CD68 (FITC) and SNRPC (Cy3) antibodies are omitted.

C: In the normal temporal cortex, NeuN<sup>+</sup> neurons are not stained upon omission of the NeuN (FITC) and SNRPC (Cy3) antibodies. \*: autofluorescence of intraneuronal lipofuscin.

D: GFAP<sup>+</sup> activated astrocytes in the temporal grey matter are not stained upon omission of the GFAP (FITC) and SNRPC (Cy3) antibodies.

E: Olig2<sup>+</sup> oligodendrocytes in the white matter are not stained upon omission of the Olig2 (FITC) and SNRPC (Cy3) antibodies.

F: CD34<sup>+</sup> endothelial cells of cortical blood vessels are not stained upon omission of the CD34 (FITC) and SNRPC (Cy3) antibody.

Microphotographs were taken with an Axiophot (Zeiss, Jena, Germany) and Zen 2 software (Zeiss). Original magnification: x400 (objective: x40). Adjustment for contrast and brightness were performed with Adobe Photoshop software version CC.

**Supplemental Figure 4** Reactivity of recAb with HEp-2 cells

Representative staining pattern of nBCR and tBCR of PCNSL #01, #02, and #10 with HEp-2 cells. NBCR of PCNSL #01 and #10 did not react, while PCNSL #02 showed a weak immunostaining compared to the positive control (human serum containing anti-nuclear antibodies). Regarding tBCR, PCNSL #01 and #02 weakly reacted with HEp-2 cells, while PCNSL #10 was negative.

Fluorescence with FITC-conjugated anti-human IgG, original magnification x400. Microphotographs were taken with an Axiophot (Zeiss, Jena, Germany) and Zen 2 software (Zeiss). Original magnification: x400 (objective: x40).

**Supplemental Figure 5** Numbers of proteins recognized in PCNSL by recAb derived from nBCR and tBCR of PCNSL

BoxPlot diagram shows the numbers of proteins that were recognized by at least one nBCR and tBCR recAb in immunoprecipitation using total protein extracts from PCNSL. Only proteins co-immunoprecipitating with either nBCR or tBCR were analysed. Statistical significance was determined by the exact Wilcoxon signed rank test (calculated with R version 3.5.0, R Foundation for Statistical Computing, Vienna, Austria).

**Supplemental Figure 6** RecAb do not bind to SAMD14 / neurabin-I in Western blot analysis

Total protein extracts from the respective PCNSL (lane 1), epilepsy tissue (lane 2), glioblastoma multiforme (lane 3), and peripheral blood mononuclear cells (lane 4) were used. RecAb were used at 50 µg/ml as first antibody, followed by FITC-conjugated anti-human IgG (5 µg/ml, Thermo Fisher). Similar results were obtained with recAb at 10 µg/ml. Arrows indicate 45 kDa (SAMD14) and 151 kDa (neurabin-I), respectively.

**Supplemental Figure 7** TBCR recognize multiple proteins as evidenced by dot blot analysis

As target, protein lysates from PCNSL cases #01 - #05, #09, and #10 (row I, A-G), from epilepsy (row II, A-G), glioblastoma multiforme (GBM, row III, A-I), and peripheral blood mononuclear cells (PBMC, row IV, A-I) were used. As controls, the respective tBCR (row V, A-G), recSA13 (loading control, row VI, A-G), and HEK293T cells (row VII, A-G) were spotted. In H and I, tetanus toxoid protein (initial concentration: 0.5 µg, Sigma) was used as target, I serves as negative control with omission of the primary antibody. TBCR and recSA13 were used at a starting concentration of 10 ng. Peroxidase-conjugated polyclonal rabbit anti-human IgG (1:25,000 Sigma) was used as secondary antibody.

**Supplemental Figure 8** Affinity of recAb derived from nBCR and tBCR for SNRPC

A: RecAb derived from PCNSL #01 to #10 were tested for binding of SNRPC by ELISA. Compared to the positive control, there is only very low binding of the recAB derived from both the nBCR as well as the tBCR. Monoclonal rabbit anti-SNRPC (clone EPR16034, Abcam) and mouse anti-MBP (clone MBP101, Abcam) served as positive and negative control, respectively. RecAb as well the positive and negative controls were used at a concentration of 0.4 ng/µl.



B: RecAb derived from PCNSL #09 was tested in serial dilutions for binding to SNRPC by ELISA. Initial concentration of all antibodies was 0.4 ng/μl. Note only a slight binding of recAb at highest concentration of the recAb. Analysis was performed in triplicate. Data represent one of three tests yielding similar results.

C: SNRPC was recognized by the recAb derived from the nBCR as well as the tBCR of PCNSL #09 only when tested at a concentration 500-fold increased to the positive control, anti-SNRPC (Abcam). Despite low-affinity, the tBCR showed increased binding as compared to the corresponding nBCR. Analysis was performed in triplicate. Data represent one of three tests yielding similar results.

**Supplemental Figure 9** Neurabin-I expression in PCNSL tissue as determined by Western Blot

Total protein extracts from 20 PCNSL (cases #31 - #50, for patients characteristics see Suppl. Table 1) were used. A tumor cell content of >80% was assured by analysis of hematoxylin & eosin-stained cryostat sections above and below the tissue sections used for protein extraction. Jurkat cells (J) served as positive control recommended by the manufacturer showing a strong band at 151 KDa (arrows), corresponding to neurabin-I. M: marker. As primary antibodies, two different polyclonal antibodies against the N-terminus of neurabin-I were used, i.e. rabbit anti-neurabin-I (1:500, antibody online, ABIN2790677, A) and rabbit anti-neurabin-1 (1:500, antibody online, ABIN1108406, B). HRP-conjugated goat anti-rabbit (1:4000, ThermoFisher, Waltham, MA) was used as secondary antibody.

Rabbit anti-human transferrin receptor (1:500, clone HPA028598, Sigma) and Ponceau staining were used as loading control.

**Supplemental Figure 10** Neurabin-I is expressed in CNS neurons and their axons

A,B: In the normal temporal cortex, neurabin-I (Cy3) is expressed in the cytoplasm of NeuN<sup>+</sup> (FITC) neurons (arrowheads). An elongated swollen axon in the temporal grey matter also expresses neurabin-I (Cy3) (B, arrows).

C: In the frontal cortex, large neurons characterized by a prominent nucleolus (arrowheads) as well as their axons (arrows) express neurabin-I (Cy3).

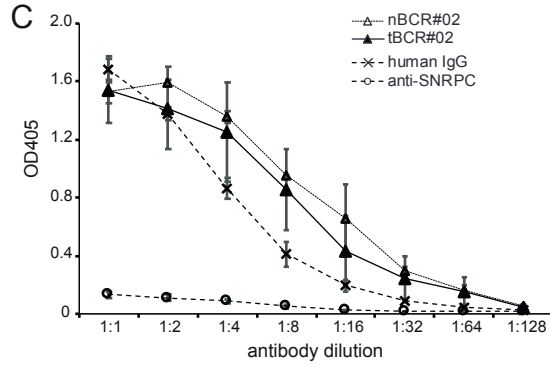
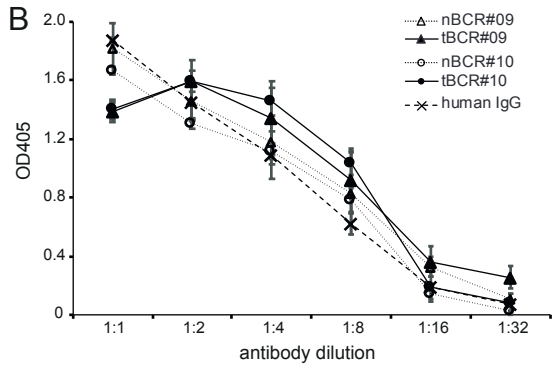
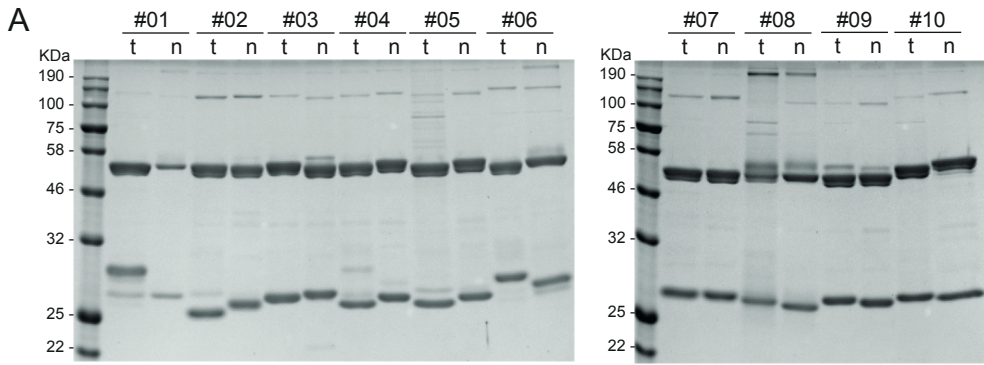
D: Omission of the anti-neurabin-I and anti-NeuN antibodies abolishes Cy3 and FITC staining from neurons. \*: autofluorescence of intraneuronal lipofuscin.

Microphotographs were taken with an Axiophot (Zeiss, Jena, Germany) and Zen 2 software (Zeiss). Original magnification: x400 (C, D), x1000 (A, B). Adjustment for contrast and brightness were performed with Adobe Photoshop software version CC.

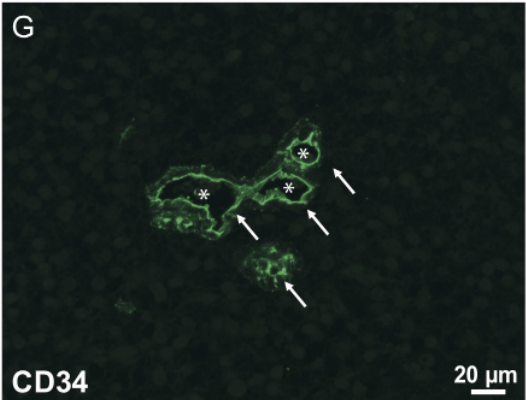
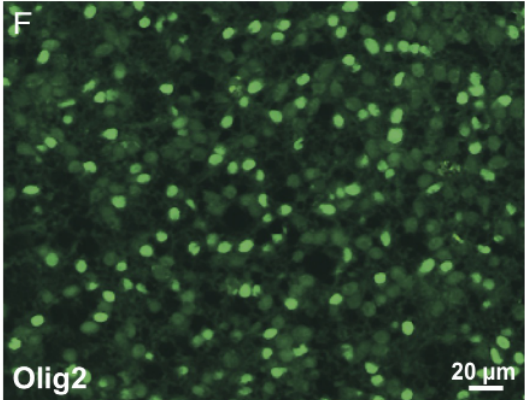
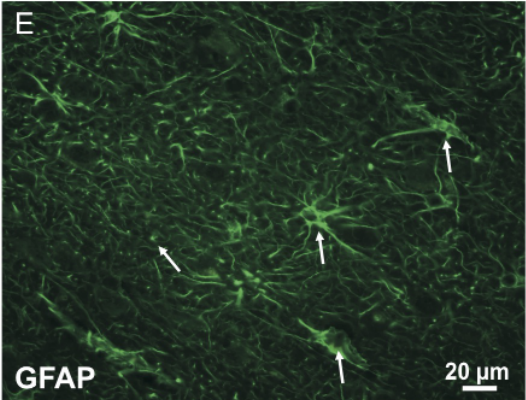
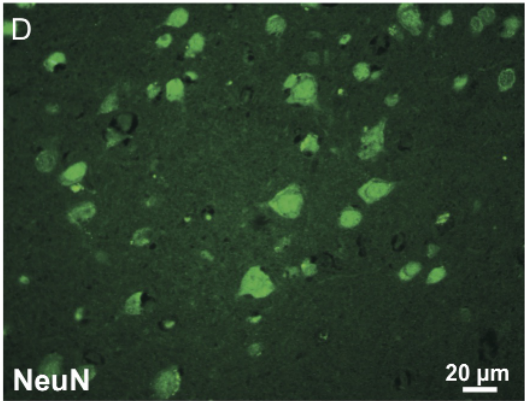
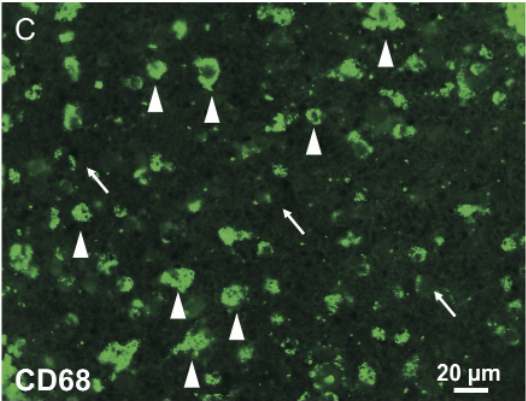
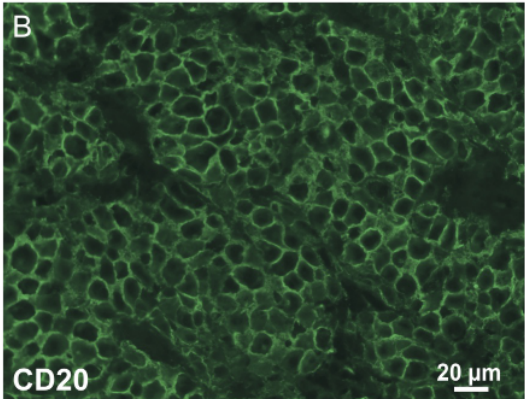
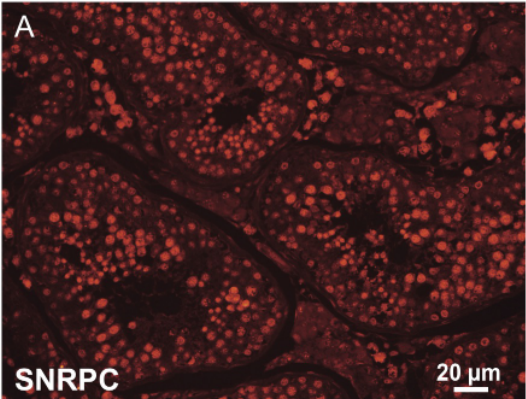
### **Supplemental Figure 11** Model for the impact of a faulty GC reaction on PCNSL pathogenesis

Instead of normal B cell maturation with SHM of a naïve B cell resulting in a terminally differentiated plasma/memory B cell (upper panel), a mutation prevents apoptosis of an auto-/polyreactive B cell, instead conferring a survival advantage. Upon GC entry, SHM starts, modifying *IG* and *BCL6* genes. Through extension of SHM to proto-oncogenes (aberrant SHM, ASHM) and the occurrence of translocations, the B cell acquires further oncogenic hits while simultaneously becoming unable to stop SHM. This leads to increased auto-/polyreactivity without being (further) selected for high-affinity BCR antigen binding, thus, resulting in a PCNSL (precursor) B cell characterized by a GC exit geno-/phenotype with auto-/polyreactivity with a shift towards increased numbers of CNS proteins recognized.

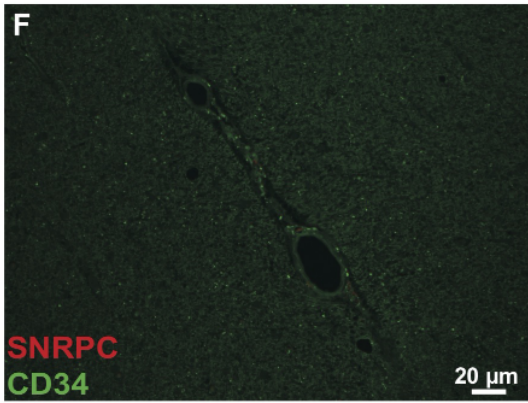
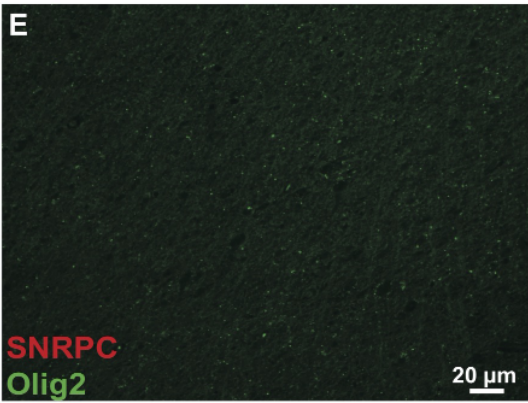
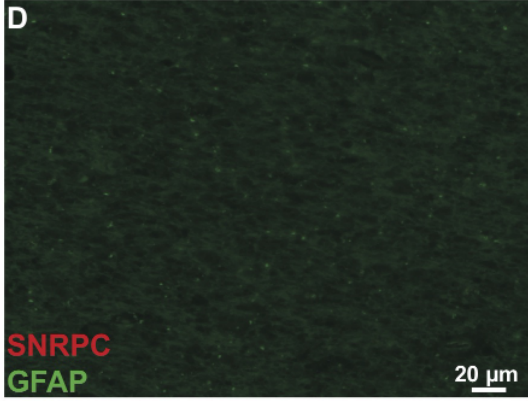
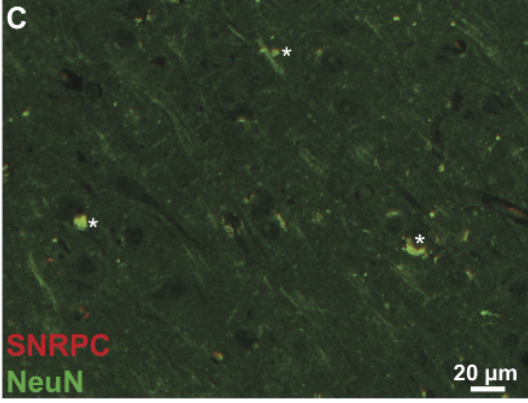
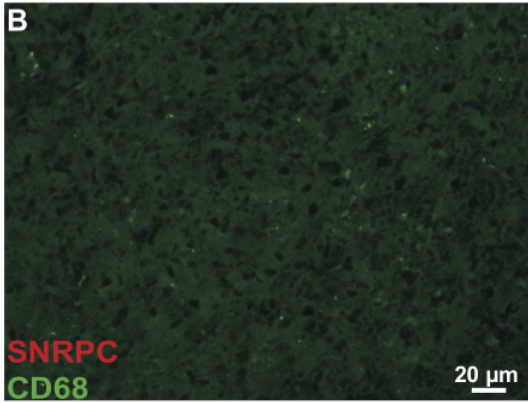
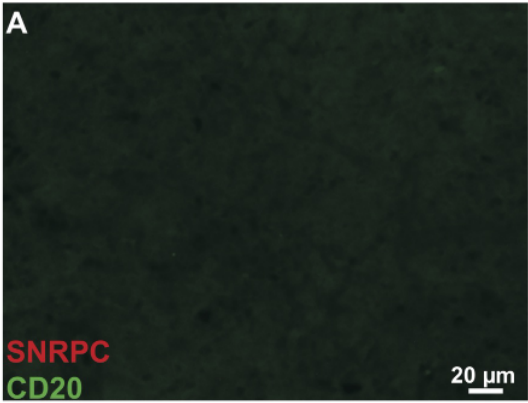
# Supplementary Figure 1



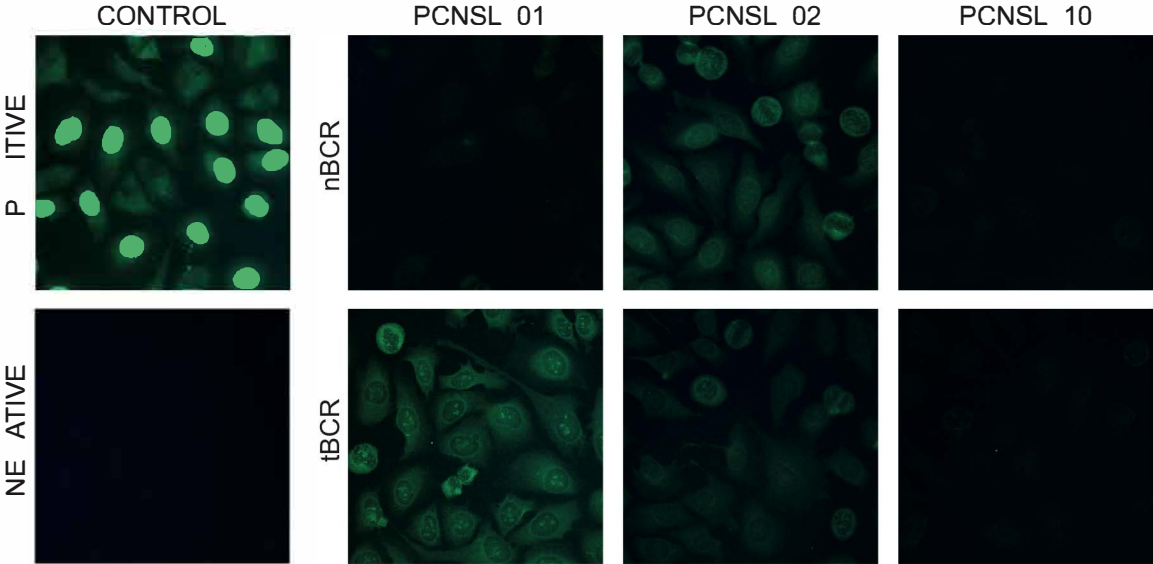
Supplementary Figure 2



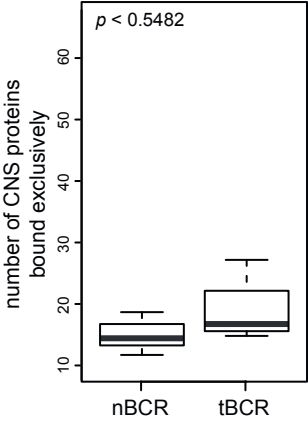
Supplementary Figure 3



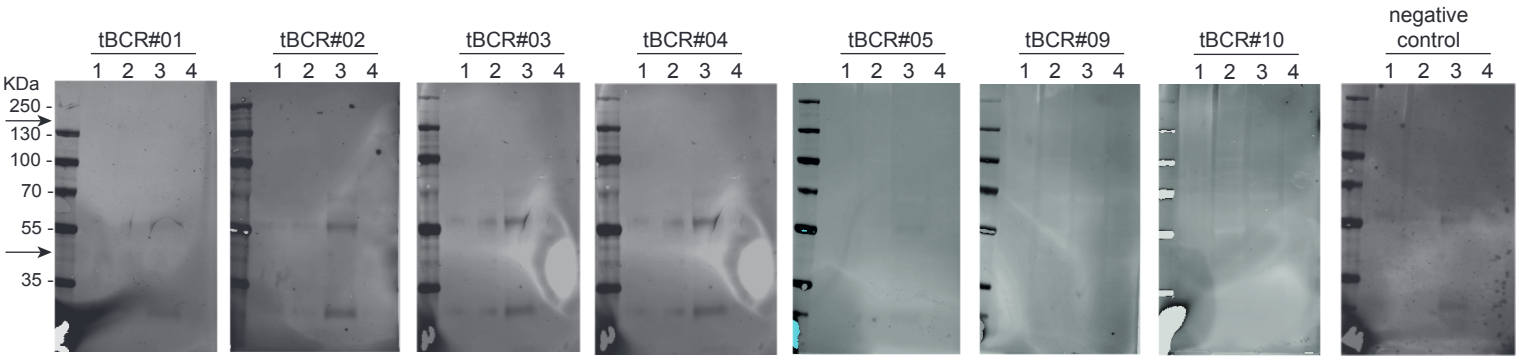
Supplementary Figure



Supplementary Figure 5

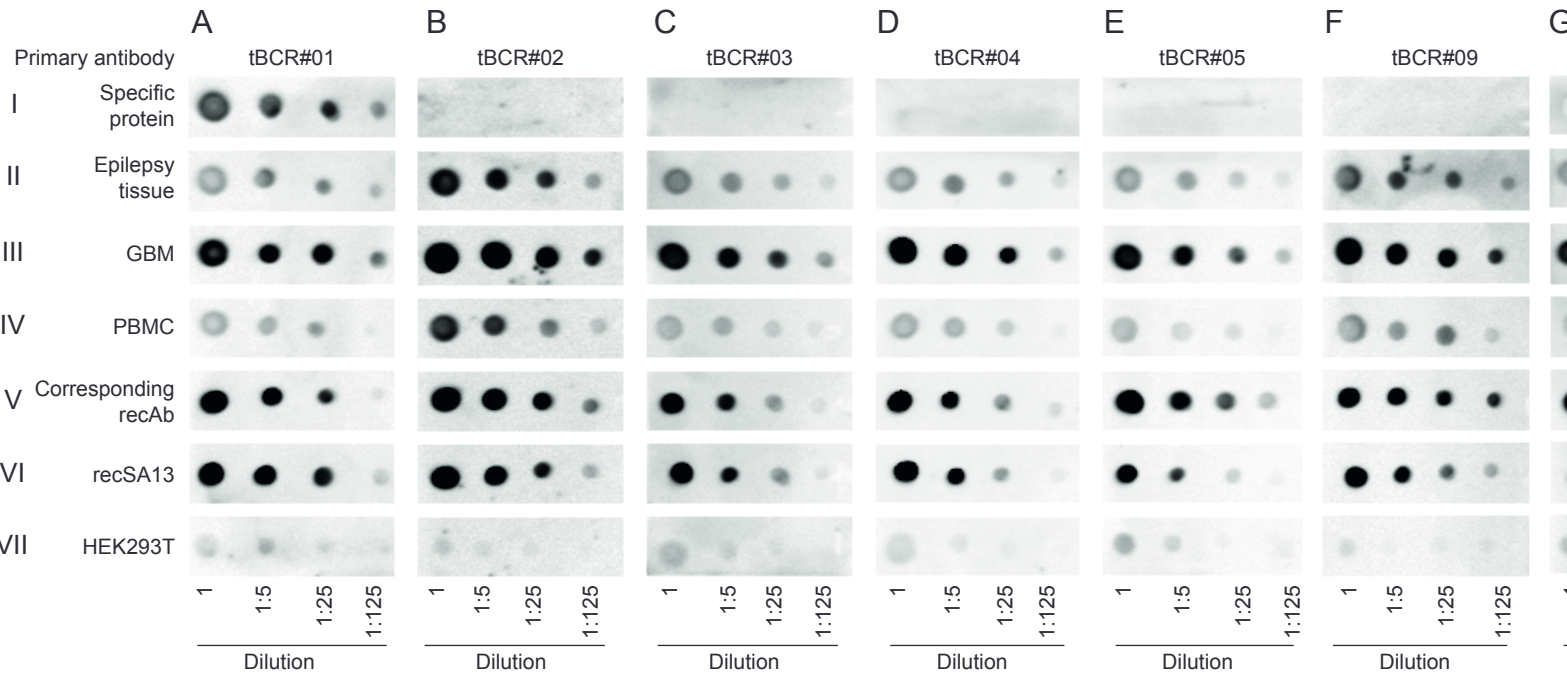


Supplementary Figure 6



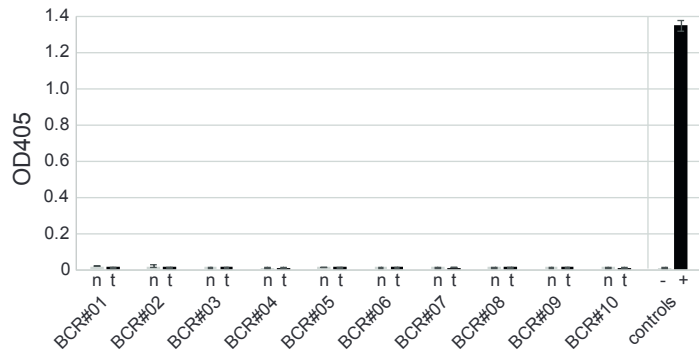


Supplementary Figure 7

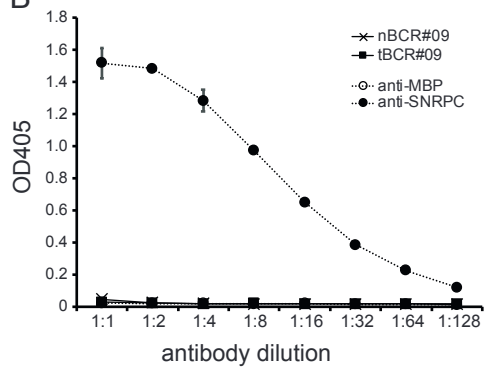


# Supplementary Figure 8

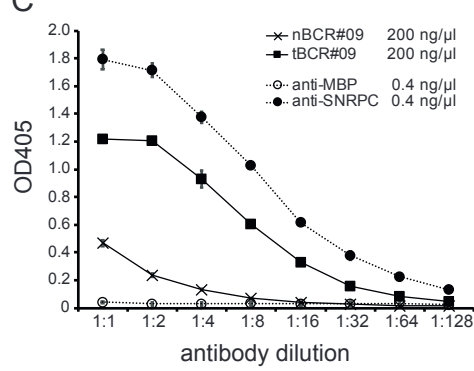
A



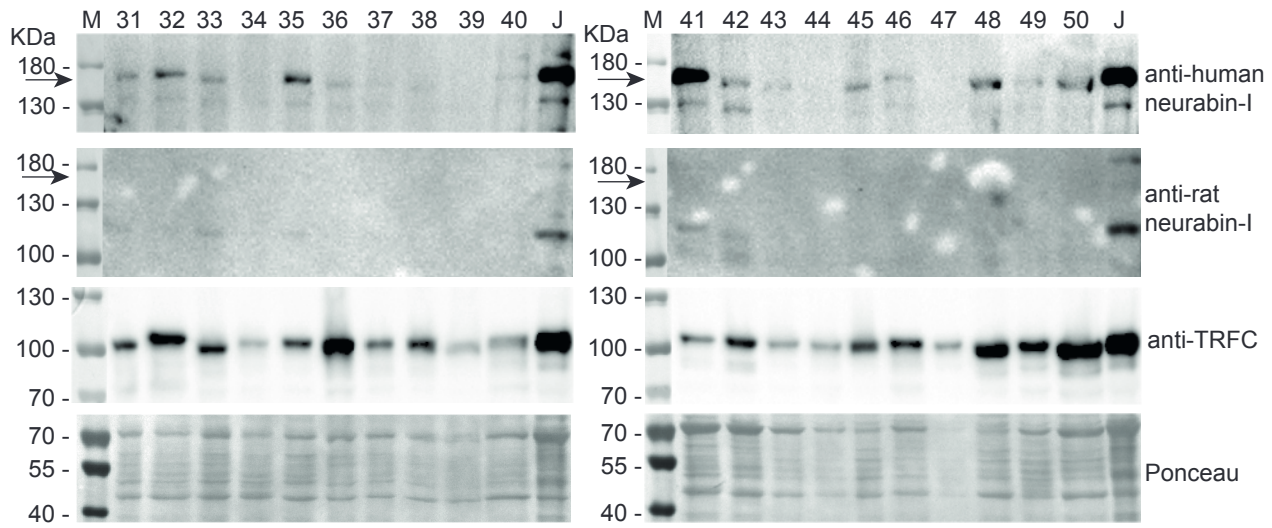
B

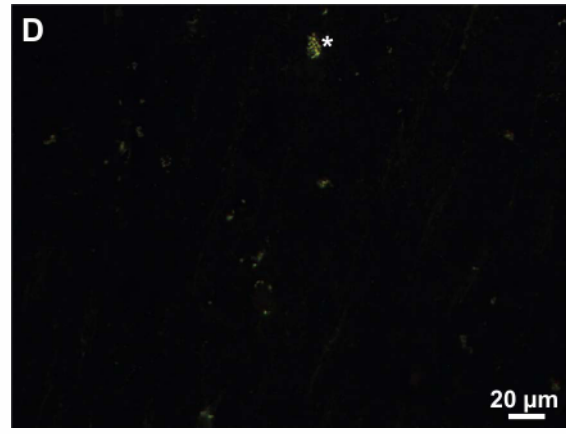
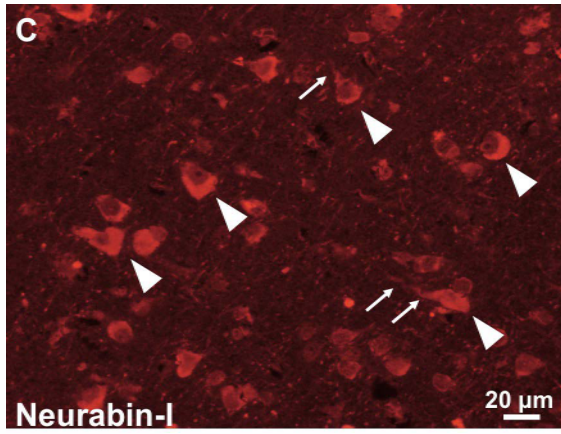
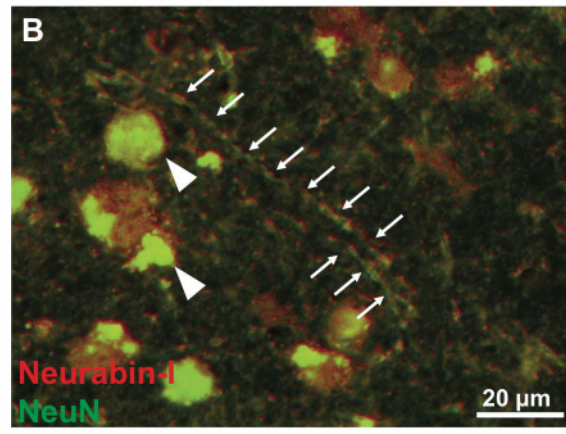
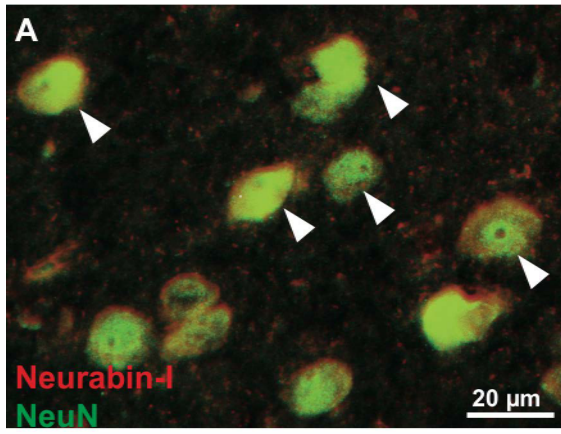


C



Supplementary Figure 9





Supplementary Figure 11

